Microporous and Mesoporous Materials 119 (2009) 97–103

Contents lists available at ScienceDirect

Microporous and Mesoporous Materials

journal homepage: www.elsevier.com/locate/micromeso

Room temperature ionic liquids as templates in the synthesis of mesoporous silica via a sol–gel method

Juan Zhang [a,b], Yubo Ma [a,b], Feng Shi [a], Lequan Liu [a,b], Youquan Deng [a,*]

[a] Centre for Green Chemistry and Catalysis, Lanzhou Institute of Chemical Physics, Chinese Academy of Sciences, Lanzhou 730000, China
[b] Graduate University of Chinese Academy of Sciences, Beijing 100049, China

ARTICLE INFO

Article history:
Received 3 May 2008
Received in revised form 17 September 2008
Accepted 6 October 2008
Available online 11 October 2008

Keywords:
Confined
Ionic liquid
Mesoporous
Silica gel
Sol–gel

ABSTRACT

With various RTILs as templates, amorphous mesoporous silica gel materials were synthesized according to a proper sol–gel method. The materials display pore diameter of 3–12 nm, pore volume of 0.4–1.3 cm^3/g and BET surface area of 300–800 m^2/g. The effect of variations of the anions and cations of ILs, the alkyl chain length on imidazolium cation and IL concentration in the reaction system on the pore structure and thermal stability of the silica gel materials was preliminarily studied. It is suggested that, the pore size of silica gel can be tuned by variations of ILs and IL content. The different kind of the anions of ILs could largely impact the properties of the obtained silica gel materials. The mesoporous silica gels with 1-alkyl-3-methylimidazolium tetrafluoroborate as templates possessed larger pore sizes of 5–12 nm and higher thermal stability than the materials obtained with other ILs as templates.

1. Introduction

Porous materials have become more and more important in either science or technology. They can be grouped into three classes based on their pore diameter (d): microporous, $d < 2.0$ nm; mesoporous, $2.0 < d < 50$ nm; macroporous, $d > 50$ nm. Among them, mesoporous materials have attracted more attention due to tailoring ability of the pore structure over a wide range, and the potential applications in catalysis, separations, nanoelectronics, sensors, and spacial host materials for substances or reactions [1]. In the synthesis of uniform mesoporous materials, various templates have been employed [2–9]. In detail, templating by individual molecules, micelles, and emulsions or latex particles can gives rise to mesopores. Since 1992, various surfactants, ionic [10–13] or neutral [13,14], as templates, have been introduced to direct the formations of mesopores in the material based on hydrothermal or sol–gel methods.

Room temperature ionic liquids (RTILs) have received considerable attentions in many areas of chemistry and industry due to their superior properties such as high thermal stability, nonflammability, and essentially zero vapor pressure [15–17]. However, their potential as templates and reaction media for nanocomposite materials is relatively less reported. As a new kind of templates, ILs can be recycled more easily, which is considered to be economical and environmental friendly. In addition, the great diversity of ILs may not only enrich the organic template family but also lead to porous materials with novel structure and properties. Meanwhile, nanoporous materials with ILs supported or templated had also potential applications in catalysis and separations [18,19]. Thus, it is valuable to carry out investigations on the synthesis and properties of ILs templated porous materials. During the past decade, 1-alkyl-3-methylimidazolium salts with Cl^- and Br^- anions (C_nMImCl and C_nMImBr, where $n = 2–18$) have been used as templates in mesoporous material synthesis according to hydrothermal crystallization procedure, and the results suggested that ILs performed in a similar manner to the alkyltrimethylammonium family of templates [20]. A variety of ILs, C_nMImCl, were used as templates to prepare monolithic, super-microporous silica with lamellar order via the nanocasting technique, displaying a very regular structure with *ca.* 1.2–1.5 nm in pore diameter [21]. So far, the majority of the reports are focused on the ILs with long alkyl side chain on the imidazolium cation and halide anions [20–25], which could direct the formation of mesophase in the synthesis system to produce well-ordered microporous and mesoporous materials. $BMImBF_4$, a short-chain IL was used as the template to produce monolithic mesoporous silica with wormhole framework via a convenient sol–gel nanocasting technique [26]. The properties of ILs can be notably changed with variations of cation and anion. Thus, the diversity of the selected ILs as the template in sol–gel synthesis can have important effect on the properties of the obtained porous materials. However, RTILs with varied composed cations and an-

* Corresponding author. Fax: +86 931 4968116.
E-mail address: ydeng@lzb.ac.cn (Y. Deng).

1387-1811/$ - see front matter © 2008 Published by Elsevier Inc.
doi:10.1016/j.micromeso.2008.10.003

ions as templates to synthesize porous materials are less reported yet [27].

In this work, according to a proper sol–gel method, various RTILs with RMIm (R, alkyl) and Th cation and BF_4, NTf_2, $N(CN)_2$, CF_3SO_3 (Scheme 1) as a new kind of recyclable templates were employed in the synthesis of mesoporous silica gel materials. In addition, the effect of the variation of ILs, the IL template content on the pore structure and thermal stability of silica gel was also investigated herein.

2. Experimental

2.1. Materials and reagents

All chemicals used in the experiments were of analytical grade, and were used without further purification. Silver dicyanamide $AgN(CN)_2$ was purchased from Aldrich and used as received.

2.2. Synthesis of ILs

$BMImBF_4$, $HMImBF_4$, $OMImBF_4$, $BMImNTf_2$, $BMImCF_3SO_3$, $BMImN(CN)_2$ were synthesized and purified according to the literature [17]. S-butylthiophene dicyanamide $BThN(CN)_2$ was synthesized in our lab through following procedure: S-butyltetrahydrothiophene chloride was prepared with high yield from the reaction of tetrahydrothiophene and appropriate amount of chlorobutane in acetone. Silver dicyanamide $AgN(CN)_2$, (4.0 g, 11 mmol) was added to a solution of BThCl (5.2 g, 11 mmol) in water (60 ml), and the resulting suspension was stirred for 24 h. Then the filtrate was evaporated under vacuum. The obtained crude compound was dissolved in dichloromethane and the solution was dried over anhydrous magnesium sulphate. Finally, the colorless $BThN(CN)_2$ was obtained by subjecting the liquid to a higher vacuum to eliminate volatile components.

2.3. Preparation of IL incorporated nanocomposites (IL-sg) and silica gel materials (wsg-IL)

IL (0.05–1.0 g) was dissolved into the solution of tetraethyl orthosilicate (5.00 ml) and ethanol (2.50 ml) and was stirred for 2 h under 40 °C. Then the solution was cooled to room temperature into which 2.50 ml hydrochloride aqueous solution (mixture of 10.00 ml distilled water and 1.00 ml 37% concentrated hydrochloride acid) was added dropwise under vigorous stirring. After 5 h, the solution was exposed to a vacuum at 60 °C for 2 h for the removal of the ethanol solvent during which a transparent gel was formed. Then after the gel was aged for 12 h in air at 60 °C, the obtained materials with different IL loading in mass were subjected to a higher vacuum at 80 °C for 5 h to eliminate the volatile components. The loadings of ILs were calculated through the ratio of the mass of the ILs initially employed to the total amount of IL-sg materials finally obtained.

IL-sg was washed with mixture of ethanol and acetone (v/v, 1:1) under refluxing for 6 h and this procedure was repeated for at least thrice for the vigorous washing of IL, and then was filtrated. The solid of silica gel was dried at 80 °C under higher vacuum for 5 h, denoted as wsg-IL.

2.4. Characterizations and instruments

BET surface area, average pore volume, and average pore diameter of the porous silica gel materials were measured by physisorption of N_2 at 77 K over a Micromeritics ASAP 2010. Before

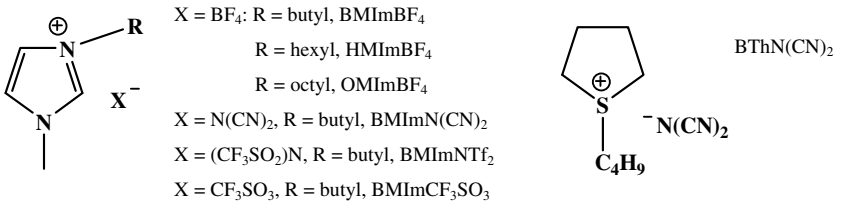

Scheme 1. RTILs templates involved in the synthesis of mesoporous silica gel materials.

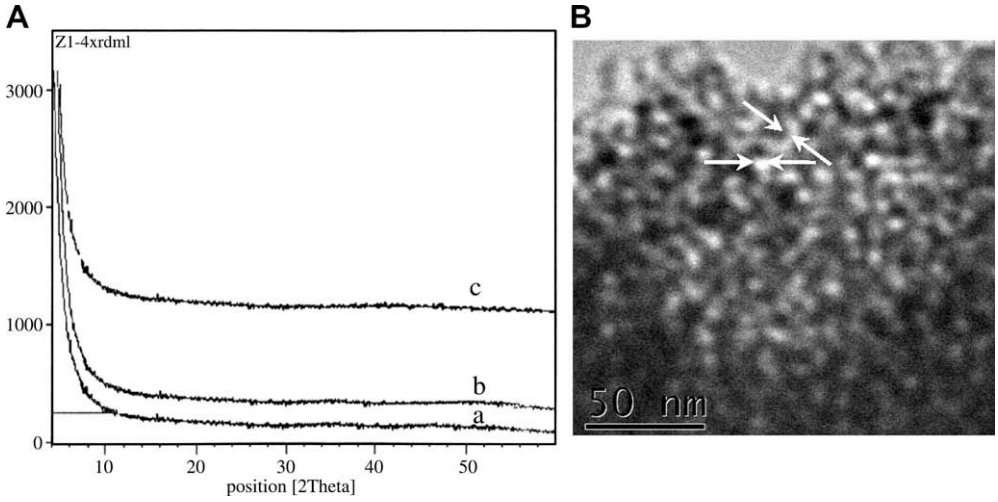

Fig. 1. (A) XRD patterns of wsg-$BMImBF_4$ with $BMImBF_4$ loading of: (a) 15 wt%, (b) 25 wt%, and (c) 25 wt% after being calcined at 500 °C. (B) TEM image of wsg-$BMImBF_4$ with $BMImBF_4$ loading of 15 wt%.

measurement, the samples were degassed at 80 °C for 10 h to remove the moisture and adsorbed gases. The isotherms were elaborated according to the BET (Brunauer, Emmett and Teller) method for surface area calculation, and pore size distribution curves derived from the desorption branches for the porous silica gel materials with BJH (Barrett–Joyner–Halenda) methods.

X-ray diffraction (XRD) patterns were performed on a Siemens D/max-RB powder X-ray diffractometer. Diffraction patterns were recorded with Cu Ka radiation (40 mA, 40 kV) over a 2θ range of 1–60° at a scan rate of 2°/min.

TEM images were obtained using a JEOL JEM-100CXII transmission electron microscope. Samples were grounded in a mortar and then suspended in toluene under ultrasonic. One droplet of the suspension was applied to a 400-mesh carbon-coated copper grid and dried in air before measurement.

3. Results and discussion

Silica gel materials were obtained by vigorous washing of the nanocomposites of IL-sg with ethanol solvent. Then wsg-IL was

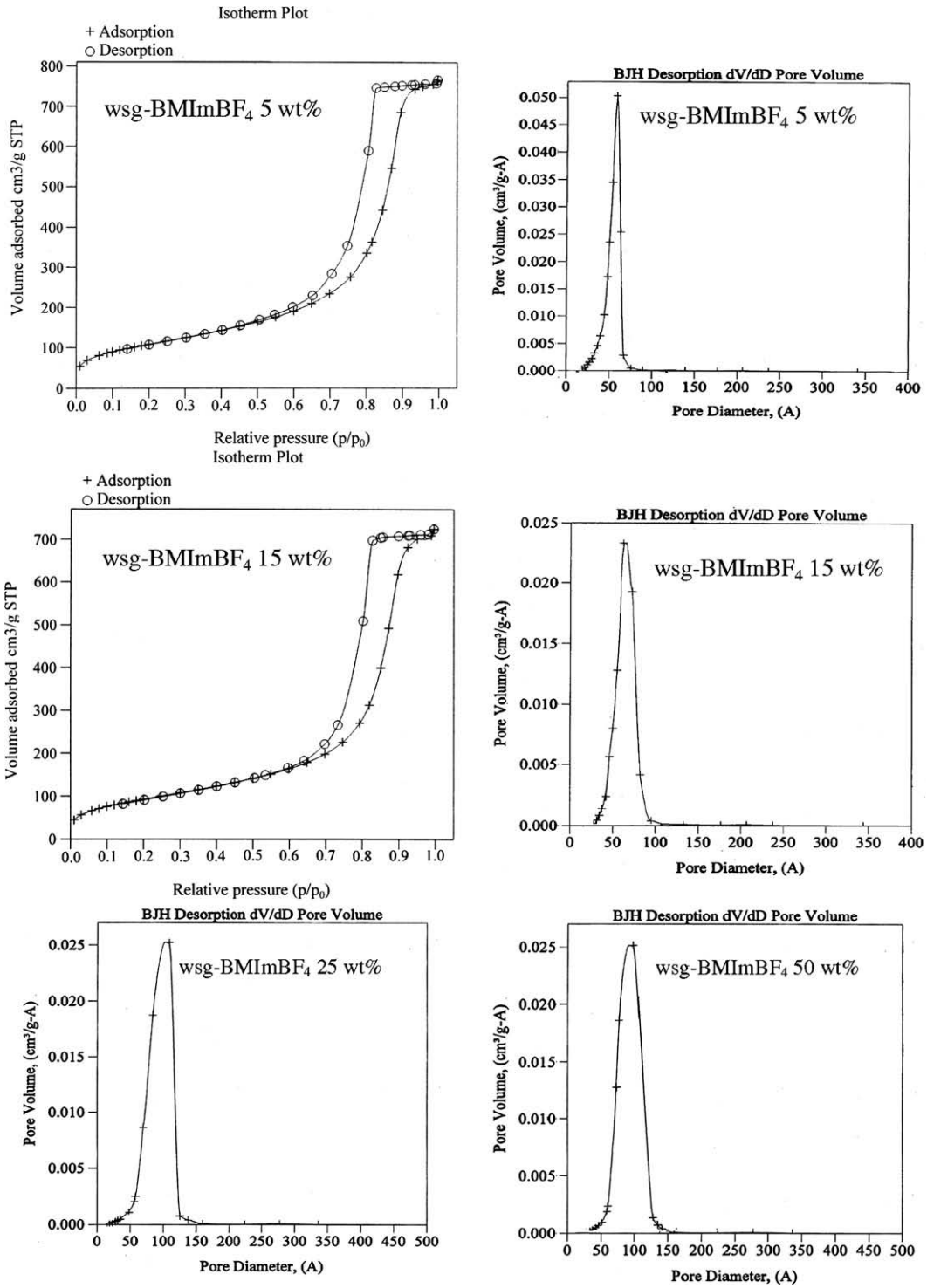

Fig. 2. N_2 gas adsorption–desorption isotherm and pore size distribution plots of wsg-$BMImBF_4$ with varied IL loadings.

characterized by FTIR spectra (Figs. S1, S2, S3), in which the adsorption bands characteristic for ILs could not be observed compared with the spectra of IL-sg, indicating that ILs could be almost totally removed by extraction of IL-sg with mixed solvent repeatedly. Meanwhile, after washing, ILs in the solvent could be easily recycled simply by distillation. XRD characterizations in Fig. 1 do not show any clue for the formation of crystallized silica, indicating that the silica gel materials obtained with $BMImBF_4$ and $BMImNTf_2$ as templates was amorphous, even after being calcined at 500 °C. In accordance with other ILs such as $HMImBF_4$, $OMImBF_4$, $BMImN(CN)_2$, $BMImCF_3SO_3$, and $BThN(CN)_2$ as templates, the obtained silica gels based on the same synthesizing method were all amorphous. The TEM image shown in Fig. 1 exhibits a disordered wormhole-like pore structure, which is consistent with the XRD result. The pore size estimated by TEM analysis is around 8 nm.

N_2 adsorption–desorption isotherms and size distribution plots of wsg-$BMImBF_4$ with $BMImBF_4$ loading from 5 to 50 wt% (Fig. 2) show a Type IV isotherm with a large hysteresis indicating a 3D intersection network of porous structure according to IUPAC explanations [28,29], and capillary condensation of N_2 occurs at relative pressure p/p_0 of *ca.* 0.75. As shown in Table 1 and Fig. 3, all the wsg-$BMImBF_4$ with varied IL content were characterized to be mesoporous with average pore diameter in the range of 5–11 nm and BET surface areas of 300–400 m^2/g. With $BMImBF_4$ loading of 5 wt%, the average pore diameter, pore volume and BET surface area of wsg-$BMImBF_4$ were 5.9 nm, 0.8 cm^3/g and 390 m^2/g, respectively. With IL loading being increased to 15 and 25 wt%, the average pore diameter of wsg-$BMImBF_4$ was increased correspondingly between 7.6 and 10.4 nm. It is suggested that, the pore size of the silica gel enlarged considerably with $BMImBF_4$ loading increasing from 5 to 25 wt%. However, with further increasing of $BMImBF_4$ loading to be 38 and 50 wt%, the average pore diameter of silica gel was 10.2 and 10.6 nm, respectively, which was almost the same with the measurement of 10.4 nm with 25 wt% of $BMImBF_4$ loading. So it is suggested that the pore size of wsg-$BMImBF_4$ was not significantly affected by the variations of IL content from 25 wt% to the higher. It can be also seen that, the surface area of silica gel was the highest with the lowest IL content of 5 wt%. A narrow pore size distribution was displayed for the measurement of wsg-$BMImBF_4$ with a lower IL loading of 5 wt%, and with IL loading being increased, the pore size distribution range of wsg-$BMImBF_4$ showed a slight widening and then almost unobvious changes were observed with further increasing of IL loading from 25 to 50 wt%. Therefore, according to the above discussions, it is suggested that, the pore structure of the obtained mesoporous silica gel can be tuned by the variations of IL content in the synthesis system, especially with lower IL content, the effect was remarkable, *i.e.* pore size was increased with initial increasing of IL content, and then unvaried with further increasing of IL content.

As reported before [26], a new so-called hydrogen bond–*co*–π–π stack mechanism, responsible for the formation of the wormhole-like mesoporous silica with $BMImBF_4$ as template via the nanocasting technique, was proposed. In addition, it is believed that, hydrogen bond may be formed between BF_4^- anion and silanol, directing the oriented arrangement of the BF_4^- anions along the pore walls, and the imidazolium cation was aligned with the anion based on coulomb interactions. There also existed additional π–π stacking associations between the imidazolium cations, which were important for the directions of mesopores. The aggregations of $BMImBF_4$ along with pore walls could be formed and increased with IL content being firstly increased from 5 to 25 wt% in the formation of mesopores during reaction and ageing procedures. Thus, the pore size was increased gradually and became the largest at 25 wt%. However, when IL content was increased further, even larger associations between the imidazolium cations could not be formed, so in the process of pore formation, more and more $BMImBF_4$ cannot be confined within the pores but aggregate on the surface of the silica gel which had no effect on the pore structures of wsg-IL at the higher IL loadings. Thus, the pore size of mesoporous silica gel was initially enlarged and then almost unchanged with increasing of IL content. This trend is similar to the previous results [27,30] that further increasing of template content had unobvious effect on the pore structure of the mesoporous materials.

With $HMImBF_4$ as the template, the pore structure of wsg-$HMImBF_4$ with IL loading of 25 wt% was measured with average pore diameter of 11.1 nm, pore volume of 1.3 cm^3/g and BET

Table 1
Pore structure of wsg-IL.

wsg-IL	IL loading (wt%)	Average pore diameter (nm)	Pore volume (cm^3/g)	BET surface area (m^2/g)
wsg-$BMImBF_4$	5	5.9	0.8	390
	15	7.6	0.9	343
	25	10.4	1.1	355
	38	10.2	1.1	350
	50	10.6	1.2	345
wsg-$HMImBF_4$	25	11.1	1.3	371
wsg-$OMImBF_4$	25	11.2	1.3	353
wsg-$BMImN(CN)_2$	25	7.7	0.8	389
wsg-$BThN(CN)_2$	25	3.5	0.6	679
wsg-$BMImCF_3SO_3$	25	2.2	0.4	765
wsg-$BMImNTf_2$	25	3.2	0.6	662

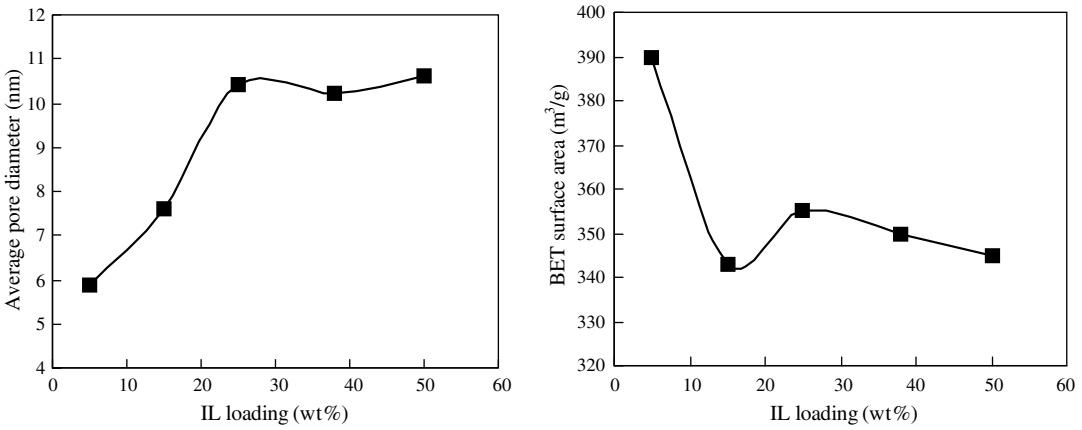

Fig. 3. Effect of IL loading on the pore size and BET surface area of wsg-$BMImBF_4$.

surface area of 371 m^2/g, suggesting that increasing the alkyl side chain length on the imidazolium cation can slightly increase the pore size of silica gel. With longer alkyl chain on the imidazolium cation, in addition of π–π stacking associations between imidazolium cations, the dispersive interactions between the longer alkyl side chain could direct the slightly larger associations between the cations, which leaded to the slightly enlarged pores in the silica gel. This is also alike the previous results that the pore sizes of mesoporous molecular sieves can be slightly tuned by the chain length using quaternary ammonium salt surfactants with different alkyl chain length, surfactants with longer chain length directed the slight larger pores of mesoporous materials [31]. However, with

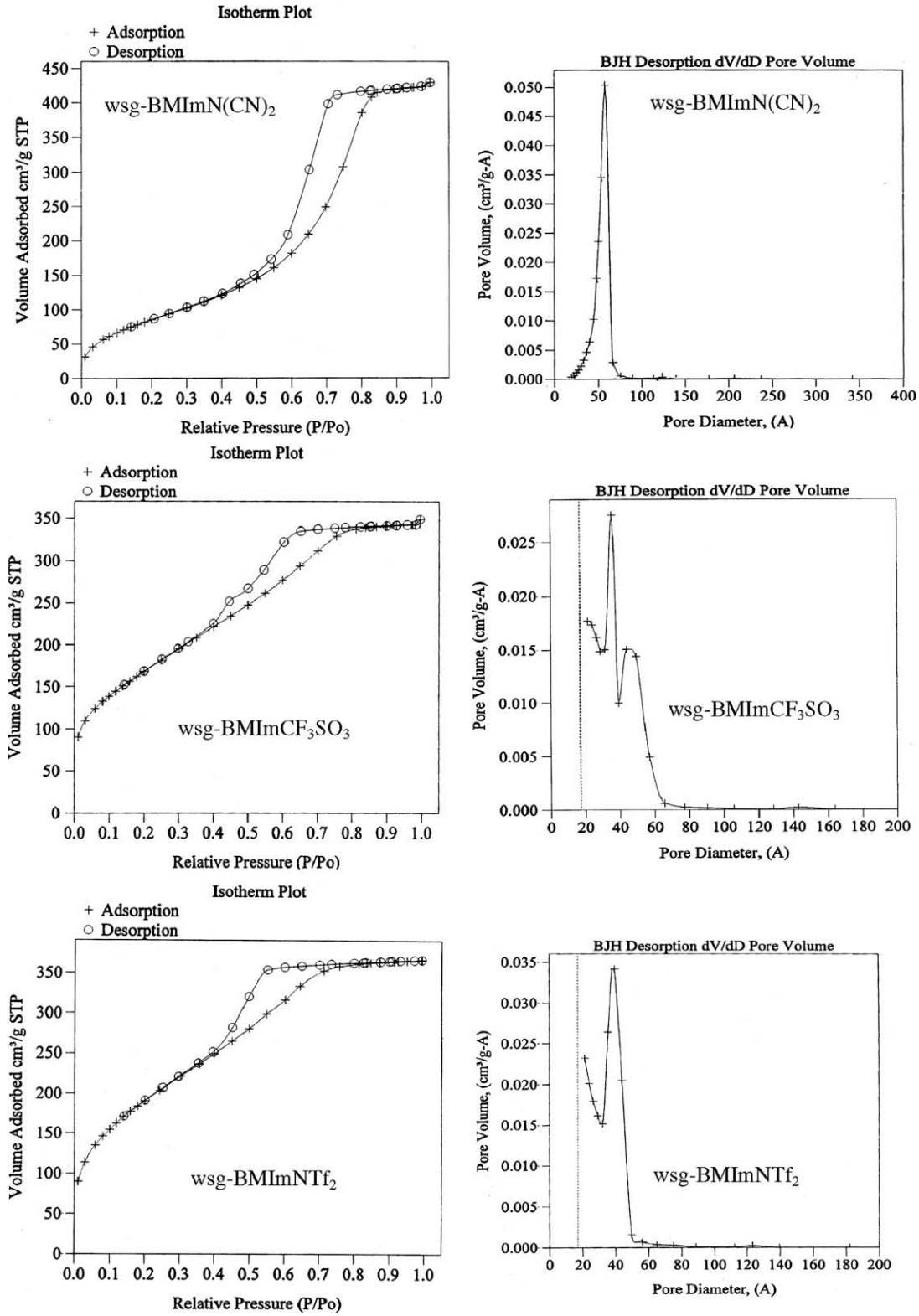

Fig. 4. N_2 gas adsorption–desorption isotherm and pore size distribution plots of wsg-IL with IL loading of 25 wt%.

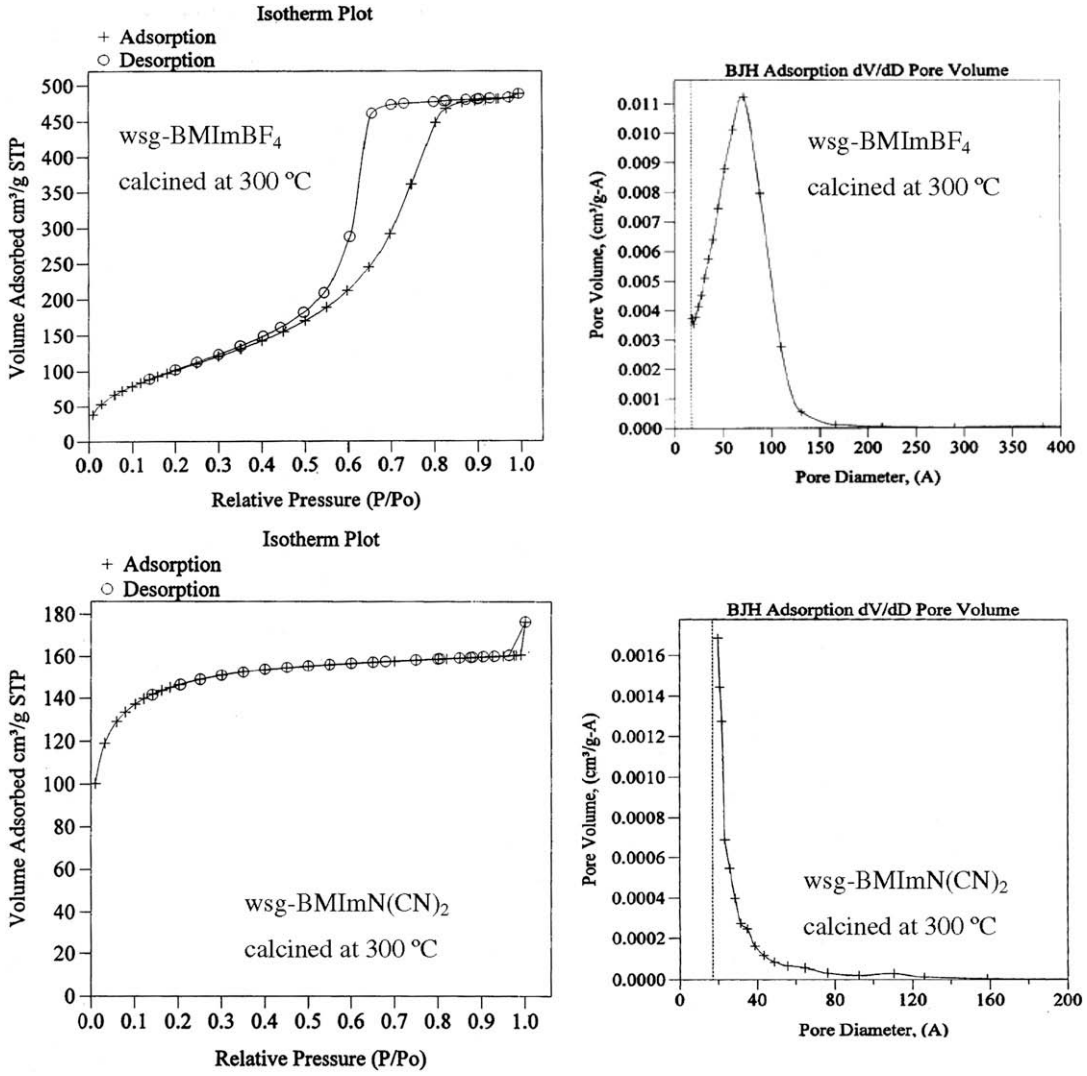

Fig. 5. N_2 gas adsorption–desorption isotherm and pore size distribution plots of wsg-IL with 1,3-dialkylimidazolium based ILs (IL loading, 25 wt%) after calcination at 300 °C for 10 h.

further increasing of the chain length, *i.e.* when $OMImBF_4$ was used, there were not obvious changes in the pore structure of silica gel as indicated by the similar measurements for wsg-$OMImBF_4$ compared with wsg-$OMImBF_4$ in Table 1.

With 1-butyl-3-methylimidazolium based ILs as templates, the effect of the variation of anion moiety on the pore structure of silica gel was also studied. As indicated in Fig. 4, used different ILs as templates with IL loading of 25 wt%, remarkably different type of N_2 adsorption–desorption isotherms and pore size distribution plots were displayed. It is suggested that, varied anions resulted in the remarkably different pore structure of silica gel materials. With $BMImN(CN)_2$ as template, wsg-$BMImN(CN)_2$ showed the similar N_2 adsorption–desorption isotherm of Type IV to wsg-$BMImBF_4$, while it displayed a comparatively narrower pore size distribution range than wsg-$BMImBF_4$. The average pore diameter and pore volume of wsg-$BMImN(CN)_2$ was 7.7 nm and 0.8 cm^3/g, respectively, smaller than the measurements of 10.4 nm and 1.1 cm^3/g for wsg-$BMImBF_4$. When $BMImCF_3SO_3$ and $BMImNTf_2$ were used as templates, the pore structure of the obtained silica gel materials were similar to each other, which exhibited characteristics of both the adsorption isomers of Types I and IV, and a large hysteresis loop of Type II could be also observed. This suggests that, there were considerable micropores in the two silica gel materials. The average pore diameter of wsg-$BMImCF_3SO_3$ and wsg-$BMImNTf_2$ was 2.2 and 3.2 nm, respectively, smaller than the obtained silica gel materials used $BMImN(CN)_2$ and $BMImBF_4$ as templates. In addition, BET surface area of wsg-$BMImCF_3SO_3$ and wsg-$BMImNTf_2$ was 765 and 662 m^2/g, respectively, larger than that of wsg-$BMImN(CN)_2$ and wsg-$BMImBF_4$. Thus, the pore size of the silica gel obtained by 1-butyl-3-methylimidazolium salts with different anions as templates follows: $BF_4^- > N(CN)_2^- > NTf_2^- \sim CF_3SO_3^-$, and the surface area was ranked in the opposite order. The strength of the hydrogen bonds between water molecules and anions increases in the order $BF_4^- < NTf_2^- < CF_3SO_3^-$ [32], thus stronger hydrogen bond interactions of the anions of NTf_2^- and $CF_3SO_3^-$ with silica gel may decrease the interactions between the anion and imidazolium cation. Additionally, NTf_2^- and $CF_3SO_3^-$ are

Table 2
Pore structure of wsg-IL (IL loading, 25 wt%) after calcination at 300 °C for 10 h.

wsg-IL	Average pore diameter (nm)	Pore volume (cm^3/g)	BET surface area (m^2/g)
wsg-$BMImBF_4$	5.8	0.7	296
wsg-$BMImBF4$[a]	4.9	0.4	236
wsg-$BMImN(CN)_2$	3.0	0.1	20
wsg-$BMImCF_3SO_3$	2.5	0.4	579
wsg-$BMImNTf_2$	2.6	0.3	398

[a] Calcination at 500 °C for 10 h.

larger than BF_4^-, therefore, π–π stackings of imidazolium rings were blocked and weakened resulting in the relatively disordered arrangement of ILs in the reaction system. Thus, wsg-$BMImCF_3SO_3$ and wsg-$BMImNTf_2$ with considerable micropores in the silica gel materials can be obtained.

Then the imidazolium ring was changed to be BTh which was a sulfur-contained cation with the absence of π delocalized electrons, and $BThN(CN)_2$ was used as template to synthesize porous silica gel. The result in Table 1 shows that, wsg-$BThN(CN)_2$ had the average pore diameter of 3.5 nm, smaller than wsg-$BMImN(CN)_2$, and the surface area of the former was larger than that of the latter. In the case of wsg-$BMImN(CN)_2$, π–π stacking interactions between imidazolium cations exist and this is important for the self-assembly of ILs to direct the formation of mesopores in the silica gel. However, BTh is a cation without π-delocalized electrons, and there are not π–π stacking interactions between BTh cation itself. Therefore, wsg-$BThN(CN)_2$ has dramatically different pore size and surface area compared with wsg-$BThN(CN)_2$. Based on the above results, it can be concluded that, by selecting IL templates with different composed cation and anion moiety, the pore structure can be largely tuned, and the mesoporous silica gel materials with a wide range of pore size from 3 to 12 nm in diameter can be obtained.

Hereafter, the thermal stability of the mesoporous silica gel materials used various IL as templates with IL loading of 25 wt% was investigated. According to the measurement results in Fig. 5 and Table 2, it is shown that, calcination at 300 °C could lead to the dramatic decrease of surface area of all the obtained mesoporous silica gel materials because the pore collapse was inevitably occurred during calcination process. With different IL templates, the heat treatment had different effect on the pore structure of calcined silica gel. The most serious decreasing of pore structure can be found for wsg-$BMImN(CN)_2$ by the fact that, after calcination, surface area of silica gel was only 20 m^2/g compared with 389 m^2/g before calcination. Wsg-$BMImN(CN)_2$ calcined at 300 °C showed a characteristic Type I adsorption isomer without a hysteresis loop observed in Fig. 5, indicating that almost all the pores in the silica gel were collapsed and nonporous material was obtained after calcination, and this is also confirmed by the fact that no peaks can be observed in the corresponding pore size distribution plot in Fig. 5. With $BMImCF_3SO_3$ and $BMImNTf_2$ as templates, after calcination, there was not so obvious decrease of pore sizes as was measured for wsg-$BMImN(CN)_2$. However, after calcination, the surface area of wsg-$BMImNTf_2$ and wsg-$BMImCF_3SO_3$ was dramatically decreased by 264 and 186 m^2/g, respectively. With $BMImBF_4$ as template, before calcination, the average pore diameter, pore volume and surface area of the silica gel were 10.4 nm, 1.1 cm^3/g and 355 m^2/g, respectively. After calcination at 300 °C for 10 h, the measured values were decreased to 5.8 nm, 0.7 cm^3/g and 297 m^2/g, respectively. It also showed a decrease of pore size resulted from collapse of mesopores in wsg-$BMImBF_4$. However, it is interesting that, wsg-$BMImBF_4$ after calcination at 300 °C still exhibited Type IV adsorption isomer indicating the presence of the considerable amount of mesopores in the calcined silica gel. Meanwhile, the pore size distribution range (2–16 nm) showed a widening compared with the measurement (5–12 nm) without calcination as shown in Fig. 2. After being calcined at 500 °C for 10 h, the measurement values for wsg-$BMImBF_4$ were 4.9 nm in average pore diameter and 236 m^2/g in surface area, suggesting that pore structure of wsg-$BMImBF_4$ was still not dramatically changed. Therefore, it can be concluded that, wsg-$BMImBF_4$ displayed the best thermal stability among the materials with various IL as templates. The thermal stability of the silica gel materials obtained with different ILs as template followed: wsg-$BMImBF_4$ > wsg-$BMImCF_3SO_3$ > wsg-$BMImNTf_2$ > wsg-$BMImN(CN)_2$.

4. Conclusion

With various RTILs as recyclable templates, amorphous mesoporous silica gel materials were synthesized according to a proper sol–gel method. The materials displayed pore diameter of 3–12 nm, pore volume of 0.4–1.3 cm^3/g and BET surface area of 300–800 m^2/g. Variation of the anions of ILs had a dramatic effect on the pore structure of the obtained silica gel materials. The average pore diameter of the silica gel with different ILs as template followed: wsg–$BMImBF_4$ > wsg-$BMImN(CN)_2$ > wsg-$BThN(CN)_2$ ~ wsg-$BMImNTf_2$ > wsg-$BMImCF_3SO_3$. Increasing the alkyl chain length on the imidazolium cation resulted in a slight increase of the pore size of the silica gel. The pore size of the silica gel increased initially and then did not significantly change with increasing of IL content. Calcination at a higher temperature caused collapse of the mesopores in the materials. The mesoporous silica gel with $BMImBF_4$ as template has comparatively better thermal stability.

Acknowledgement

This work was financially supported by National Natural Science Foundation of China (Nos. 20533080 and 20503037).

Appendix A. Supplementary data

Supplementary data associated with this article can be found, in the online version, at doi:10.1016/j.micromeso.2008.10.003.

References

[1] A. Stein, Adv. Mater. 15 (2003) 763.
[2] A. Corma, Chem. Rev. 97 (1997) 2373.
[3] C.T. Kresge, M.E. Leonowicz, W.J. Roth, J.C. Vartuli, J.S. Beck, Nature 359 (1992) 710.
[4] R. Liu, Y. Shi, Y. Wan, Y. Meng, F. Zhang, D. Gu, Zh. Chen, B. Tu, D. Zhao, Am. Chem. Soc. 128 (2006) 11652.
[5] A. Imhof, D.J. Pine, Nature 389 (1997) 948.
[6] Q. Huo, D.I. Margolese, U. Ciesla, P. Feng, T.E. Gier, P. Sieger, R. Leon, P.M. Petroff, F. Schüth, G.D. Stucky, Nature 368 (1994) 317.
[7] H. Yang, N. Coombs, G.A. Ozin, Nature 386 (1997) 692.
[8] S.S. Kim, W. Zhang, T.J. Pinnavaia, Science 282 (1998) 1302.
[9] H.Y. Zhu, J.-C. Zhao, J.W. Liu, X.Z. Yang, Y.N. Shen, Chem. Mater. 18 (2006) 3993.
[10] H. Yang, A. Kuperman, N. Coombs, S. Mamiche-Afara, G.A. Ozin, Nature 379 (1996) 703.
[11] A.D. Firouzi, D. Kumar, L.M. Bull, T. Besier, P. Sieger, Q. Huo, S.A. Walker, J.A. Zasadzinski, C. Glinka, J. Nicol, D. Margolese, G.D. Stucky, B.F. Chmelka, Science 267 (1995) 1138.
[12] Q. Huo, R. Leon, P.M. Petroff, G.D. Stucky, Science 268 (1995) 1324.
[13] S.A. Bagshaw, E. Prouzet, T.J. Pinnavaia, Science 269 (1995) 1242.
[14] P.T. Tanev, T.J. Pinnavaia, Science 267 (1995) 865.
[15] K.R. Seddon, Nat. Mater. 2 (2003) 363.
[16] T. Welton, Chem. Rev. 99 (1999) 2071.
[17] P. Wasserscheid, T. Welton, Ionic Liquids in Synthesis, Wiley-VCH Weinheim, New York, 2003.
[18] F. Shi, Q. Zhang, D. Li, Y. Deng, Chem. Eur. J. 11 (2005) 5279.
[19] C.P. Mehnert, R.A. Cook, N.C. Dispenziere, M. Afeworki, J. Am. Chem. Soc. 124 (2002) 12932.
[20] C.J. Adams, A.E. Bradley, K.R. Seddon, Aust. J. Chem. 54 (2001) 679.
[21] Y. Zhou, M. Antonietti, Chem. Mater. 16 (2004) 544.
[22] Y. Zhou, M. Antonietti, Chem. Comm. (2003) 2564.
[23] D. Kuang, T. Brezesinski, B. Smarsly, J. Am. Chem. Soc. 126 (2004) 10534.
[24] N. Žilková, A. Zukal, J. Čejka, Micropor. Mesopor. Mater. 95 (2006) 176.
[25] K. Zhu, F. Požgan, L. D'Souza, R.M. Richards, Micropor. Mesopor. Mater. 91 (2006) 40.
[26] Y. Zhou, J.H. Schattka, M. Antonietti, Nano Lett. 4 (2004) 477.
[27] K.S. Yoo, T.G. Lee, J. Kim, Micropor. Mesopor. Mater. 84 (2005) 211.
[28] K.S.W. Sing, D.H. Everett, R.A.W. Haul, L. Moscou, R.A. Pierotti, J. Rouquerol, T. Siemieniewska, Pure Appl. Chem. 57 (1985) 603.
[29] J. Rouquerol, D. Avnir, C.W. Fairbridge, D.H. Everett, J.H. Haynes, N. Pericone, J.D.F. Ramsay, K.S.W. Sing, K.K. Unger, Pure Appl. Chem 66 (1994) 1739.
[30] B. Smarsly, D. Kuang, M. Antonietti, Colloid Polym. Sci. 282 (2004) 892.
[31] Q. Huo, D.I. Margolese, G.D.Stucky, Chem, Mater. 8 (1996) 1147.
[32] L. Cammarata, S.G. Kazarian, P.A. Salter, T. Welton, Phys. Chem. Chem. Phys. 3 (2001) 5192.